Surface diffusion and desorption kinetics for perfluoronbutane on Ru(001)

M. V. Arena, E. D. Westre, and S. M. George

Citation: The Journal of Chemical Physics **94**, 4001 (1991); doi: 10.1063/1.460676
View online: http://dx.doi.org/10.1063/1.460676
View Table of Contents: http://scitation.aip.org/content/aip/journal/jcp/94/5?ver=pdfcov
Published by the AIP Publishing

Surface diffusion and desorption kinetics for perfluoro-*n*-butane on Ru(001)

M. V. Arena, E. D. Westre, and S. M. George
Department of Chemistry, Stanford University, Stanford, California 94305

(Received 27 August 1990; accepted 1 November 1990)

The surface diffusion and desorption kinetics for perfluoro-*n*-butane on Ru(001) were examined using laser-induced thermal desorption (LITD) and temperature programmed desorption (TPD) techniques. The surface diffusion displayed Arrhenius behavior and was coverage independent. The surface diffusion parameters for perfluoro-*n*-butane on Ru(001) were $E_{dif} = 2.9 \pm 0.3$ kcal/mol and $D_0 = 5.9 \times 10^{-2 \pm 0.2}$ cm^2/s. The desorption parameters for perfluoro-*n*-butane on Ru(001) were $E_{des} = 13.8 \pm 0.6$ kcal/mol and $\nu_{des} = 2.8 \times 10^{21 \pm 0.1}$ s^{-1}. In comparison, the surface diffusion parameters for *n*-butane on Ru(001) were $E_{dif} = 3.5 \pm 0.2$ kcal/mol and $D_0 = 1.4 \times 10^{-1 \pm 0.2}$ cm^2/s. The desorption parameters for *n*-butane on Ru(001) were $E_{des} = 11.9 \pm 0.5$ kcal/mol and $\nu_{des} = 3.6 \times 10^{15 \pm 0.1}$ s^{-1}. The corrugation ratio, defined as $\Omega \equiv E_{dif}/E_{des}$, was determined to be $\Omega = 0.21$ for perfluoro-*n*-butane on Ru(001). This corrugation ratio was substantially different than the corrugation ratio of $\Omega \approx 0.30$ measured for *n*-butane and various other *n*-alkanes, cycloalkanes and branched alkanes on Ru(001). The comparison between perfluoro-*n*-butane and the other alkanes indicates that fluorination lowers the surface corrugation ratio on Ru(001). Likewise, fluorination significantly increases the preexponential for desorption from Ru(001). This study illustrates the magnitude of substituent effects on surface diffusion and desorption kinetics for a physisorbed molecule on a single-crystal metal surface.

I. INTRODUCTION

Surface diffusion plays a central role in surface dynamics and surface reaction kinetics.[1-3] Surface mobility can be used to measure the characteristics of the underlying adsorbate–surface and adsorbate–adsorbate potentials. The adsorbate–surface potential can be examined by temperature-dependent surface diffusion measurements at low surface coverage. If adsorbate–adsorbate interactions are present, these interactions can be quantified by measuring the surface diffusion coefficient versus coverage.

Laser-induced thermal desorption (LITD) techniques have recently been developed as a useful method to measure surface diffusion on macroscopic single-crystal surfaces.[4-21] One of the advantages of LITD investigations is their ability to identify and quantify the diffusing adsorbate using mass spectrometric detection. Consequently, the effects of coverage, coadsorbates, additives, and isotopic substitution on surface diffusion have been explored using LITD techniques. Many of these LITD studies have focused on hydrogen[4-9] and carbon monoxide[10,11] on the Ru(001) surface.

Recent LITD studies have also examined the temperature and coverage-dependent diffusion of various physisorbed alkanes on Ru(001). This work has focused on *n*-alkanes,[12] pentane isomers,[13] cycloalkanes,[14] and tetramethylsilane[15] on Ru(001). These investigations revealed a constant corrugation ratio Ω between the diffusion activation barrier and the desorption activation barrier for these physisorbed molecules. This corrugation ratio was $\Omega \equiv E_{dif}/E_{des} \approx 0.3$ for all the alkanes on Ru(001).

The ubiquitous corrugation ratio of $\Omega \approx 0.30$ for all the hydrocarbons studied on Ru(001) indicated a strong similarity between these physisorbed molecules. The observation of a constant corrugation ratio also raised a variety of additional questions. For example, do all physisorbed molecules display a corrugation ratio of $\Omega \approx 0.30$? What effect do changes of substituent atoms have on the corrugation ratio? These were the central questions that motivated this investigation of perfluoro-*n*-butane on Ru(001).

Besides answering fundamental issues concerning the corrugation ratio, this study of perfluoro-*n*-butane on Ru(001) is also relevant because fluorinated molecules have widespread use in chemistry. Fluorinated alkanes are useful as nonpolar solvents and refrigerant fluids. Fluorinated ethers are widely employed as surface lubricants and model studies of fluorinated ethers on Ru(001) have recently been performed.[22,23] Consequently, an understanding of the physical properties of fluorinated molecules on Ru(001) is scientifically and technologically important.

By substituting fluorine atoms for the hydrogen atoms in *n*-butane, the effect of atomic substitution on surface diffusion was examined. The results demonstrated that both the surface diffusion and desorption kinetics were altered significantly upon fluorine substitution. The corrugation ratio was substantially lower for perfluoro-*n*-butane compared with *n*-butane. The desorption preexponential was also much larger for perfluoro-*n*-butane compared with *n*-butane. In this paper, these effects will be quantified and an explanation for the changes upon fluorination will be presented.

II. EXPERIMENTAL

In the LITD surface diffusion experiment,[4,16] an initial laser pulse is used to heat a well-defined area on the surface. The laser heating produces a rapid temperature jump that is

 0021-9606/91/054001-08$03.00

large enough to desorb the adsorbates within the heated area.[24,25] After a time delay, a second identical probe laser pulse heats the same area and desorbs the adsorbates that have diffused into the initially evacuated region from the surrounding surface.

The desorption flux at each delay time corresponds to the amount of diffusional refilling. The time-dependent refilling signals are then fit using the appropriate solution to Fick's second law to determine the surface diffusion coefficient.[4] This prepare-and-probe LITD experimental procedure has been employed successfully in numerous studies to measure surface diffusion on single-crystal metal surfaces.[4-21]

The experimental setup for these LITD measurements of surface diffusion has been described previously.[4] In short, the experiments were performed in an ion-pumped UHV chamber with background pressures below 3×10^{-10} Torr. Analysis of surface cleanliness and surface order was carried out with Auger electron spectroscopy (AES) using a single-pass cylindrical mirror analyzer (CMA) and low energy electron diffraction (LEED) spectrometry.

A TEM-00 Q-switched Nd:phosphate glass laser producing pulse lengths of 100–130 ns with Gaussian spatial profiles was employed.[4] The reasons for using longer pulse lengths than are typical from Q-switched lasers have been discussed previously.[26] In the present study, the laser pulse energy before entering the UHV chamber was approximately 0.15 mJ/pulse. The pulses were focused by a 65 cm focal length lens to give a Gaussian spatial profile of 120 μm (FWHM) at the focus of the lens.

The surface was positioned at the focus of the lens. The angle between the incoming laser pulses and the surface normal was 54°. Consequently, the desorption areas were elliptical with an aspect ratio of 1.7. The dimensions of the desorption spots using the spatial autocorrelation method[16] were approximately 100 μm in diameter along the minor axis and 170 μm in diameter along the major axis.

Perfluoro-*n*-butane was adsorbed onto the Ru(001) surface using a glass capillary array doser. The doser was positioned $\approx$2 cm from the Ru(001) surface. The doser produced consistent coverages as determined by TPD analysis. The surface coverages were defined with respect to the TPD signal corresponding to the saturated monolayer coverage. The coverages were uniform to within $\pm$ 15% across the surface using LITD spatial measurements.

The surface cleaning procedure involved exposing the Ru(001) single crystal surface to a background pressure of 2×10^{-8} Torr of O_2 while cycling the temperature between 1100 and 1370 K several times. Repeated flashing to 1570 K then removed excess oxygen.[4-15] This cleaning procedure was conducted after each experiment. The surface cleanliness was monitored using both AES and CO TPD peak temperatures as discussed previously.[10-12] Argon ion sputtering and annealing cycles were necessary on a daily basis to obtain consistent results.

Hydrocarbons have been observed to be unstable in the presence of electrons.[27] Stray electrons from the ionizer of the mass spectrometer are one source of energetic electrons. Consequently, the Ru(001) crystal was biased to $-$ 80 V to repel any stray electrons for all the LITD and TPD experiments.

For each surface diffusion experiment, the Ru(001) single crystal was cleaned, dosed at a lower temperature and subsequently heated to the desired experimental temperature. A matrix of 8 to 24 desorption spots was created by translating the laser beam across the Ru(001) single-crystal surface. This translation was accomplished using mirrors mounted on piezoelectric translators with optical encoders. The desorption spots were always separated by at least 850 μm.

To ensure complete evacuation of the desorption area, each desorption spot was prepared with five consecutive laser pulses.[26] Each of the desorption spots was probed with a second sequence of similar laser pulses at time delays ranging from 6 to 800 s. The piezoelectric translators returned the laser to each of the desorption spots with an accuracy of $\pm$ 0.5 μm. Control experiments indicated that adsorption from the background pressure in the UHV chamber was insignificant.

The kinetics of perfluoro-*n*-butane desorption from Ru(001) were determined using the variation of heating rates method attributed to Redhead.[28] Heating rates between $\beta = 0.05$ and 7.6 K/s were produced using a temperature controller in conjunction with a voltage-programmed power supply. In all cases, the desorption of perfluoro-*n*-butane from Ru(001) followed first-order desorption kinetics. Because there was no indication that perfluoro-*n*-butane adsorption on Ru(001) was activated, adsorption and desorption were assumed to be reversible.

Surface diffusion and desorption measurements for hydrogen, carbon monoxide and various alkanes on Ru(001) have been performed on several Ru(001) crystals cut from the same boule.[4-15] These measurements have been reproducible on different Ru(001) crystals and crystals subjected to only a few laser shots and thousands of laser shots. There was no evidence from LEED, adsorption, or desorption studies for any surface defects produced by the laser surface heating of Ru(001) under the reported experimental conditions.

III. RESULTS

A. Surface diffusion measurements

1. Temperature dependence

The normalized refilling data for perfluoro-*n*-butane on Ru(001) at $\theta = 0.15\ \theta_s$ for a variety of temperatures are displayed in Fig. 1. θ_s is the coverage of the saturated perfluoro-*n*-butane monolayer on Ru(001) and should correspond to a coverage of $\theta_s \approx 3.2\times10^{14}$ molecules/cm^2.[29] The data points are not averages from several runs but are results from single prepare-and-probe sequences at various delay times. Refilling curves corresponding to constant diffusion coefficients were fit to the experimental data and are shown as solid lines.

To determine the value of the surface diffusion coefficient, the size of the desorption area must be known. Measurements of the LITD hole size for perfluoro-*n*-butane on Ru(001) at 110 K using the spatial autocorrelation meth-

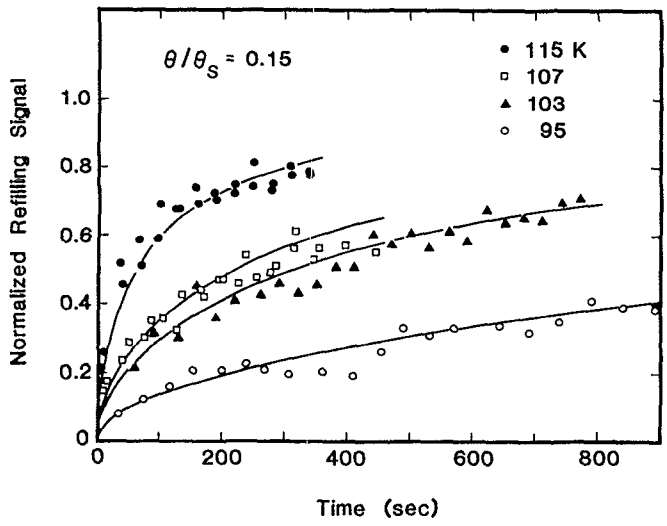

FIG. 1. Diffusional refilling data for perfluoro-*n*-butane on Ru(001) at various temperatures at $\theta = 0.15\ \theta_s$. Solid lines represent refilling curves corresponding to constant surface diffusion coefficients.

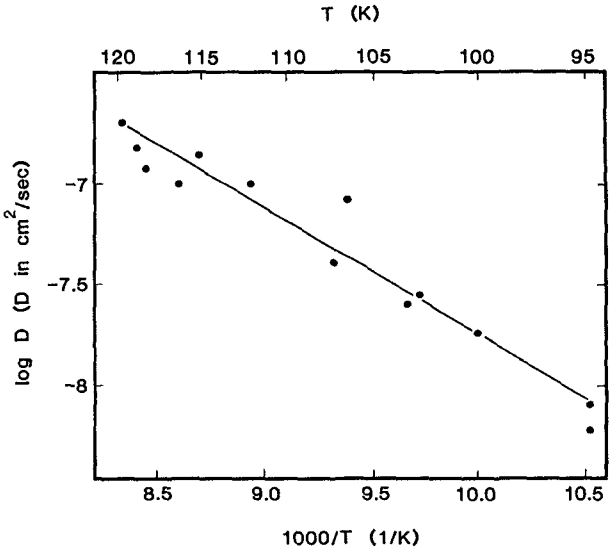

FIG. 3. Arrhenius plot of the surface diffusion coefficients for perfluoro-*n*-butane on Ru(001) at $\theta \approx 0.15\ \theta_s$. The measured surface diffusion kinetic parameters were $E_{dif} = 2.9 \pm 0.3$ kcal/mol and $D_0 = 5.9 \times 10^{-2 \pm 0.2}$ cm²/s.

od[16] are displayed in Fig. 2. In the spatial autocorrelation method, the initial desorption signal is recorded. The laser beam is then translated a distance ΔX on the surface. Desorption from the region outside the area of the initial desorption region gives rise to the second desorption signal.[16] The normalized LITD signal is defined as the ratio between the second desorption signal and the initial desorption signal.

The data shown in Fig. 2 yields a hole size of 90 μm along the minor axis. Similar measurements yield a hole size of 150 μm along the major axis. Given this desorption hole size, surface diffusion coefficients can be assigned to the diffusional refilling data in Fig. 1. The Arrhenius plot for the temperature-dependent surface diffusion coefficient of perfluoro-*n*-butane on Ru(001) at $\theta = 0.15\ \theta_s$ is displayed in Fig. 3. The slope yields an activation energy for surface diffusion of $E_{dif} = 2.9 \pm 0.3$ kcal/mol. Likewise, the y intercept yields a diffusion preexponential of $D_0 = 5.9 \times 10^{-2 \pm 0.2}$ cm²/s. The uncertainties were based on the standard deviation of the slope and y intercept obtained from standard error propagation methods.

2. Coverage dependence

If adsorbate–adsorbate interactions are present, the surface diffusion coefficient may be coverage dependent.[2,3,30] These adsorbate–adsorbate interactions can be measured by LITD diffusional refilling experiments.[30] Pronounced coverage dependence was recently observed for the surface diffusion of CO on Ru(001).[10,11] This dramatic coverage dependence was attributed to repulsive, nearest-neighbor CO–CO adsorbate–adsorbate interactions.

The coverage dependence of the surface diffusion coefficient was measured for perfluoro-*n*-butane on Ru(001). Normalized diffusional refilling data were obtained at different initial surface coverages. Figure 4 displays the surface diffusion coefficient versus coverage for perfluoro-*n*-butane

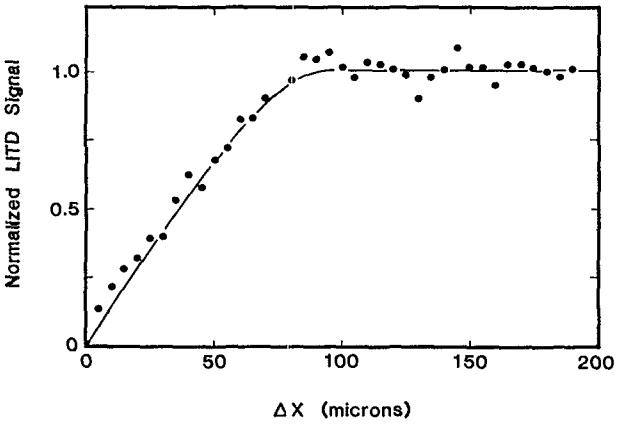

FIG. 2. Determination of the desorption hole size for perfluoro-*n*-butane at 110 K using the spatial autocorrelation method. These measurements yield a hole size of 90 μm along the minor axis of the elliptical desorption area.

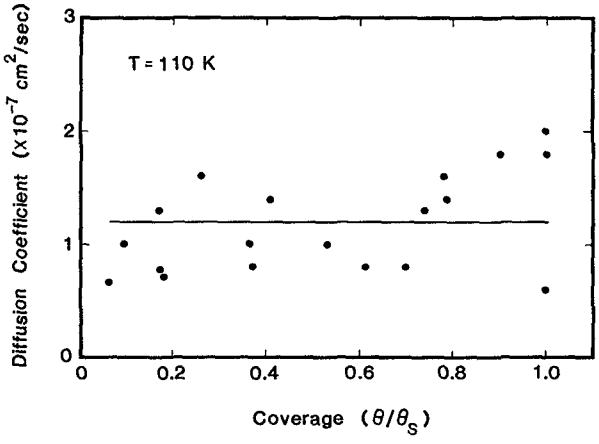

FIG. 4. Coverage-dependence of the surface diffusion coefficient for perfluoro-*n*-butane on Ru(001) at 110 K.

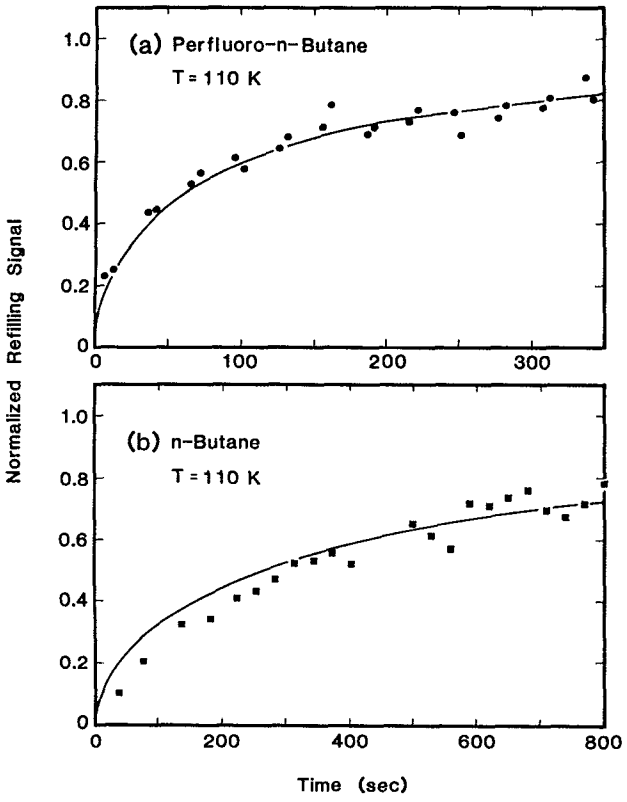

FIG. 5. (a) Diffusional refilling data for perfluoro-*n*-butane on Ru(001) at $\theta = \theta_s$ and $T = 110$ K. The measured desorption hole size was 120 μm along the minor axis. (b) Diffusional refilling data for *n*-butane on Ru(001) at $\theta = \theta_s$ and $T = 110$ K. The measured desorption hole size was 90 μm along the minor axis.

on Ru(001) at 110 K. The surface diffusion coefficient for perfluoro-*n*-butane was coverage-independent within experimental error.

3. Comparison with n-butane

The diffusional refilling curves for *n*-butane and perfluoro-*n*-butane on Ru(001) under identical experimental conditions at saturation coverage at 110 K is shown in Figs. 5(a) and 5(b). The surface diffusion coefficient for perfluoro-*n*-butane at 110 K was $D = 2.0 \times 10^{-7}$ cm^2/s. The surface diffusion coefficient for *n*-butane at 110 K was $D = 2.7 \times 10^{-8}$ cm^2/s. Consequently, the diffusion coefficient for perfluoro-*n*-butane was nearly 10 times larger than the surface diffusion coefficient for *n*-butane.

For these surface diffusion measurements, the measured desorption hole size for perfluoro-*n*-butane along the minor axis was 120 μm. This hole size was larger than the measured desorption hole size of 90 μm along the minor axis for *n*-butane under identical conditions. The larger LITD desorption area for perfluoro-*n*-butane on Ru(001) is qualitatively consistent with a larger desorption preexponential for perfluoro-*n*-butane compared with *n*-butane.[26]

B. Thermal desorption measurements

The kinetics of perfluoro-*n*-butane desorption from Ru(001) were measured using the variation of heating rates

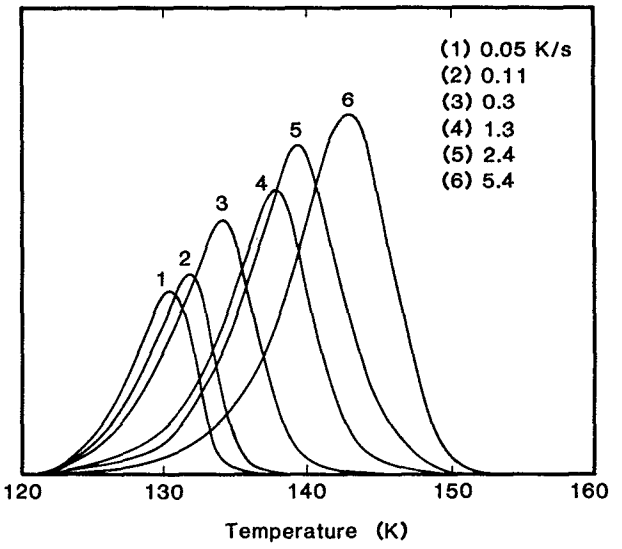

FIG. 6. Temperature Programmed Desorption (TPD) spectra for perfluoro-*n*-butane on Ru(001) as a function of heating rate. The TPD spectra have been scaled and smoothed for clarity in presentation.

method attributed to Redhead.[28] The TPD spectra corresponding to various heating rates between $\beta = 0.05$ and 7.6 K/s were recorded. A selection of these TPD spectra are shown in Fig. 6. As expected, the TPD spectra in Fig. 6 illustrate that desorption peaks with higher temperatures were obtained with faster heating rates.

The correlation between the TPD peak temperatures T_p and the heating rate β was analyzed using the standard Redhead analysis.[28] The results of this analysis are shown in Fig. 7. A desorption activation energy of $E_{des} = 13.8 \pm 0.6$ kcal/mol was obtained from the slope of this Arrhenius-like Redhead plot. In addition, a desorption preexponential of $\nu_{des} = 2.8 \times 10^{21 \pm 0.1}$ s^{-1} was determined from the y intercept and the slope. The uncertainties were based on the stan-

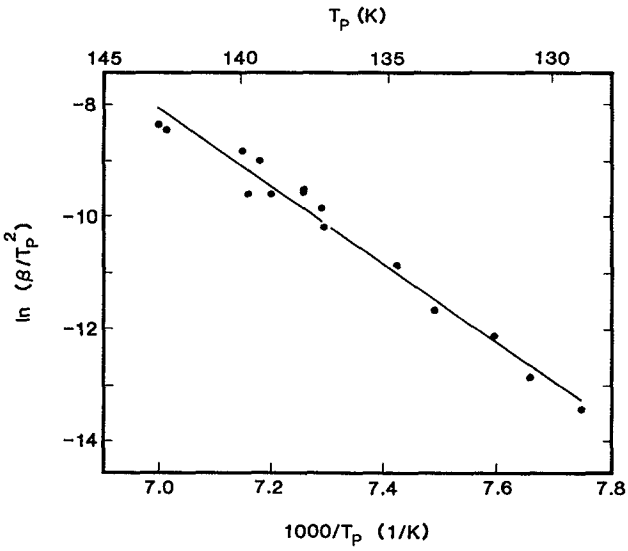

FIG. 7. Redhead analysis of the TPD spectra for perfluoro-*n*-butane on Ru(001) as a function of heating rate. The measured desorption kinetic parameters were $E_{des} = 13.8 \pm 0.6$ kcal/mol and $\nu_{des} = 2.8 \times 10^{21 \pm 0.1}$ s^{-1}.

dard deviation of the slope and y intercept obtained from standard error propagation methods.

C. Additional measurements

LEED measurements were conducted to determine if perfluoro-*n*-butane formed ordered overlayers on Ru(001). In accordance with measurements of cycloalkanes,[31-33] *n*-alkanes,[12] pentane isomers,[13] and tetramethylsilane[15] on Ru(001), no new diffraction spots were observed. However, LEED measurements of hydrocarbons are difficult to perform because of electron-induced decomposition and desorption.[27,33] LEED patterns for *n*-alkanes on single-crystal metal surfaces have only been observed for Pt(111)[27] and Ag(111).[34]

IV. DISCUSSION

A. Previous results for alkanes on Ru(001)

This study of perfluoro-*n*-butane on Ru(001) was motivated by our earlier work on a variety of alkanes on Ru(001).[12-15] The surface diffusion kinetics of the various alkanes on Ru(001) displayed uniform trends that reflected the size and degree of branching of the alkanes. For example, the diffusion activation energies scaled nearly linearly with ring size for the cycloalkanes.[14] The diffusion activation energies also scaled linearly with the hydrocarbon chain length for the straight chain *n*-alkanes.[12] In addition, the degree of alkane branching affected the diffusion activation energies. The diffusion activation energies decreased as the degree of branching increased for the pentane isomers.[13]

The desorption kinetics of the alkanes on Ru(001) also displayed uniform trends. The desorption activation energies increased with ring size and chain size for the cycloalkanes[14] and *n*-alkanes,[12] respectively. In addition, the desorption activation energy also decreased as the branching increased for the pentane isomers.[13] Given that both E_{dif} and E_{des} scaled with alkane ring size, chain size, and degree of branching, a constant corrugation ratio, $\Omega \equiv E_{dif}/E_{des}$, may be anticipated. As expected, the corrugation ratio was nearly constant at $\Omega \approx 0.30$ for all the alkanes on Ru(001).

The constant corrugation ratio indicated that a linear scaling exists between E_{dif} and E_{des} for all the alkanes on Ru(001).[12-15] The linear scaling between E_{dif} and E_{des} would not be expected unless all the alkanes shared similar binding configurations and diffusion mechanisms on Ru(001). The constancy of the corrugation ratio also argued that the alkanes were all in a similar, rigid orientation and moved in a concerted manner on the Ru(001) surface.[12-15]

Recent theoretical calculations have predicted a nearly linear scaling between diffusion and adsorption energies for *n*-alkanes, cycloalkanes, and pentane isomers physisorbed on Ru(001).[35] The calculations revealed that physisorption interactions alone were sufficient to explain the measured desorption activation energies on Ru(001). The theoretical results also predicted a constant, but smaller, corrugation ratio for all the alkanes on Ru(001).[35]

The theoretical calculations revealed similarities in the surface binding of the alkanes.[35] In general, the carbon frame of the alkanes was positioned parallel to the surface. The hydrogens that were closest to the surface were preferentially located over threefold hollow sites on Ru(001). Because fluorine has a much larger van der Waals' radius than hydrogen, this surface binding configuration suggests that substituting fluorine for hydrogen might produce a measurable effect on the surface corrugation ratio.

B. Comparison of *n*-butane and perfluoro-*n*-butane

All the kinetic parameters for the surface diffusion and desorption of *n*-butane and perfluoro-*n*-butane on Ru(001) are given in Table I. The comparison of these two molecules illustrates the effect of substituents on surface diffusion and desorption kinetics. The differences between the corrugation ratios and preexponentials should help to reveal the underlying details of surface diffusion and desorption.

1. Desorption activation energy

The desorption activation energy for *n*-butane of $E_{des} = 11.9 \pm 0.5$ kcal/mol is lower than the desorption activation energy of $E_{des} = 13.8 \pm 0.6$ kcal/mol for perfluoro-*n*-butane on Ru(001). This difference results simply from the nature of physisorption interactions. A fluorine atom is more polarizable and has more valence electrons than a hydrogen atom. Fluorine has an atomic polarizability of $\alpha = 5.5 \times 10^{-25}$ cm^3 and $n = 7.9$ effective valence electrons.[36,37] In contrast, $\alpha = 4.2 \times 10^{-25}$ cm^3 and $n = 1$ for hydrogen.[36,37] Therefore, the dispersion interactions of fluorine with the Ru(001) surface are larger and the resulting adsorption energy is higher.

Theoretical calculations were performed to predict the adsorption energies and surface binding configurations. These predictions were based on physisorption interactions obtained by the simple summing of Lennard-Jones (6–12) pair potentials for carbon–ruthenium, fluorine–ruthenium, and hydrogen–ruthenium atom–atom interactions.[35] These calculations indicated that perfluoro-*n*-butane and *n*-butane have analogous surface binding configuration on Ru(001).

TABLE I.

Molecule	E_{dif}	D_0	E_{des}	ν_{des}	E_{ads}	Ω
	kcal/mol	cm^2/s	kcal/mol	s^{-1}	kcal/mol	
perfluoro-*n*-butane	2.9 ± 0.3	$5.9 \times 10^{-2 \pm 0.2}$	13.8 ± 0.6	$2.8 \times 10^{21 \pm 0.1}$	12.8	0.21
n-butane	3.5 ± 0.2	$1.4 \times 10^{-1 \pm 0.2}$	11.9 ± 0.5	$3.6 \times 10^{15 \pm 0.1}$	12.0	0.29

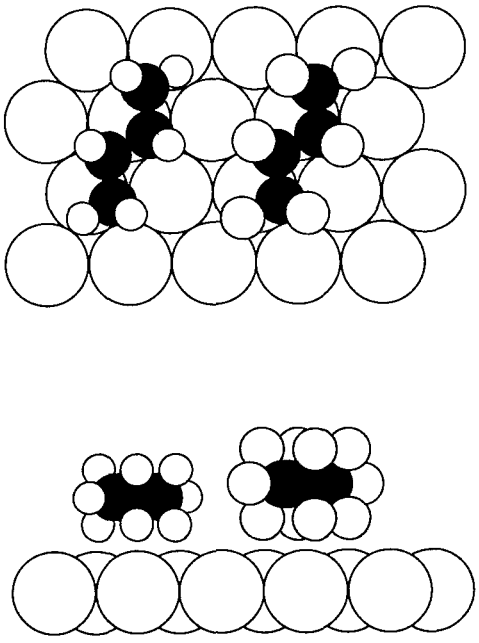

FIG. 8. Calculated binding configurations for perfluoro-*n*-butane (right) and *n*-butane (left) on Ru(001). Top and side views are presented.

For perfluoro-*n*-butane, the fluorine atoms closest to the surface are located over threefold sites. For *n*-butane, the hydrogen atoms closest to the surface are also located over threefold sites.

The predicted Ru(001) surface binding configurations based on these physisorption calculations are shown in Fig. 8. The calculated adsorption energies of perfluoro-*n*-butane and *n*-butane on Ru(001) are listed in Table I. These predicted adsorption energies agree well with the corresponding experimental desorption energies. In agreement with the earlier results for alkanes on Ru(001), physisorption interactions alone are sufficient to explain the measured desorption activation energy of perfluoro-*n*-butane on Ru(001).

2. Corrugation ratio

The diffusion activation energy for perfluoro-*n*-butane on Ru(001) was $E_{dif} = 2.9 \pm 0.3$ kcal/mol. This diffusion activation energy is smaller than the diffusion activation energy of $E_{dif} = 3.5 \pm 0.2$ kcal/mol for *n*-butane on Ru(001). The smaller diffusion barrier for perfluoro-*n*-butane of $E_{dif} = 2.9 \pm 0.3$ kcal/mol and the larger desorption activation energy of $E_{des} = 13.8 \pm 0.6$ kcal/mol combine to lower the surface corrugation ratio to $\Omega = 0.21$. This corrugation ratio is significantly lower than the corrugation ratio of $\Omega = 0.29$ for *n*-butane[12] and $\Omega \approx 0.30$ for the other alkanes on Ru(001).[12-15]

The smaller corrugation ratio for perfluoro-*n*-butane is attributed to the larger van der Waals' radius for fluorine. Fluorine has a van der Waals' radius of 1.47 Å, whereas hydrogen has a van der Waals' radius of 1.30 Å.[38] A larger atom must average its physisorption interaction over a larger area on the surface because the atom is constrained to remain farther away from the surface. Consequently, the corrugation ratio is reduced at larger distances because the molecule does not experience as great a modulation of the surface potential upon translation. The increased separation between perfluoro-*n*-butane and the Ru(001) surface is illustrated in Fig. 8. The carbon backbone of perfluoro-*n*-butane is approximately 0.48 Å farther from the plane of the surface ruthenium atoms than the carbon backbone of *n*-butane.

In addition, the corrugation ratio can be viewed in terms of the hydrogen and fluorine atoms residing in threefold sites on the Ru(001) surface. Compared with the hydrogens, the larger fluorine atom can not penetrate as deep into the high coordination, threefold sites. Subsequently, the fluorine atoms do not experience as large a modulation of the surface potential upon translation. In correspondence with the diffusion of noble gas atoms on surfaces,[38,39] the corrugation ratio is reduced as a function of the atomic radius.

The theoretical calculations based on simple physisorption interactions[35] follow the same trend as the experimentally derived corrugation ratios. The theoretical result for the corrugation ratio for perfluoro-*n*-butane on Ru(001) is $\Omega = 0.08$. In contrast, the calculated corrugation ratio for *n*-butane on Ru(001) is $\Omega = 0.10$. Although these predictions are lower than the measured corrugation ratios, the theoretical results are in qualitative agreement and predict a lower corrugation ratio for the fluorinated alkane.

3. Desorption and diffusion preexponentials

The surface diffusion and desorption preexponentials are listed in Table I. The diffusion preexponential for perfluoro-*n*-butane is somewhat smaller than the diffusion preexponential for *n*-butane. In contrast, the desorption preexponential for perfluoro-*n*-butane is orders of magnitude larger than the desorption preexponential for *n*-butane.

A transition state approach to surface desorption[40] can partially explain the large difference between the desorption preexponentials. This explanation will rely on the differences between rotational and translational partition functions for the molecules in their minimum energy binding configurations and transition states. The rotational and translational degrees of freedom will be assumed to be severely hindered in the minimum binding configuration. Consequently, the adsorbed phase partition functions for perfluoro-*n*-butane and *n*-butane will be postulated to be identical.

Rotational and translational degrees of freedom are much less hindered in the two-dimensional gas transition state for desorption. If the adsorbed phase partition functions are identical, the ratio of the desorption preexponentials will be the ratio of the partition functions for the two gas-phase molecules. According to transition-state theory, this ratio will exclude the one degree of translational freedom that represents the reaction coordinate. The vibrational degrees of freedom will also be neglected.

The moment of inertia for a molecule increases and the rotational frequency decreases as the mass of its substituent atoms increases. The rotational partition function, q_r, is proportional to $(I_A I_B I_C)^{1/2}$ where I_A, I_B, and I_C are the principle moments of inertia. Rigid body moments of inertia have been calculated from molecular configurations employed

previously.[35] With these moments of inertia for the two molecules, the calculated rotational partition function for perfluoro-*n*-butane is larger than the rotational partition function for *n*-butane by a factor of 29.

The translational partition functions will also change upon fluorine substitution. The translational partition function for one dimension q_t, is proportional to $(M)^{1/2}$ where M is the molecular mass. Given the molecular weight differences of perfluoro-*n*-butane at $m = 238$ amu and *n*-butane at $m = 58$ amu, the translational partition function for perfluoro-*n*-butane is larger than the translational partition function for *n*-butane by a factor of 4.1.

The measured desorption preexponential for perfluoro-*n*-butane is larger than *n*-butane by a factor of 93 000. Part of this difference can be accounted for by the ratio of the rotational and translational partition functions. Combining the effects of the rotational and translational degrees of freedom, the predicted desorption preexponential for perfluoro-*n*-butane is larger than *n*-butane by a factor of 120. Consequently, the total difference between the desorption preexponentials can be partially justified by the effects of fluorine substitution on the rotational and translational partition functions. Additional factors must also contribute to explain the differences between the desorption preexponentials.

The absolute magnitude of the desorption preexponential for perfluoro-*n*-butane is considerably higher than "typical" desorption preexponentials. Desorption preexponentials that are larger than $\nu_{des} \approx kT/h \approx 10^{13}$ s^{-1} have been observed by numerous authors.[41-52] Values for desorption preexponentials as high as $\nu_{des} \approx 10^{21}$ s^{-1} have been reported.[49,50] These large desorption preexponentials have been explained with transition state theory assuming: substantial dispersion in the adsorption energy;[42-44] a highly mobile transition state;[52] localized adsorption states;[45-49] and substrate reconstruction leading to changes in surface entropy.[51]

Perfluoro-*n*-butane has a lower corrugation ratio and resides further from the Ru(001) surface than *n*-butane. Consequently, perfluoro-*n*-butane may have a larger desorption preexponential because of higher mobility in the transition state.[52] In addition, the larger desorption preexponential for perfluoro-*n*-butane may be caused by dispersion in the adsorption energy.[42-44] Perfluoro-*n*-butane is a large and relatively heavy molecule that may exist in several surface binding configurations with differing adsorption energies. Unfortunately, the range of binding configurations and energies for polyatomic molecules on single-crystal surfaces is not clearly understood at this time.

The surface diffusion preexponentials are listed in Table I. Although the diffusion preexponential for perfluoro-*n*-butane is slightly smaller than the diffusion preexponential for *n*-butane, the two are nearly the same within experimental error. This similarity is striking considering the vast difference between the desorption preexponentials. The nearly equivalent diffusion preexponentials suggest that the increased mass introduced after fluorine substitution does not influence the rotational and translational degrees of freedom in the transition state for surface diffusion. This behavior implies that the diffusing molecules are much more hindered in the transition state for diffusion compared with the transition state for desorption.

The diffusion preexponentials observed for perfluoro-*n*-butane, *n*-butane and other alkanes on Ru(001) are larger than the diffusion preexponentials typically obtained for atomic diffusion.[1-3] Multiple-site hopping was introduced earlier as an explanation for these large surface diffusion preexponentials.[12] In the context of a random walk model where $D_0 = r^2\nu/4$, jump lengths of $r = 40$–50 Å were required to obtain the correct magnitude of the surface diffusion preexponential.[12] This estimate assumed attempt frequencies of $\nu = s/l$ where s is the frustrated translational velocity and l is the effective confinement length for the alkanes in their surface binding wells.[12]

Although multiple-site hopping may provide an explanation for the large diffusion preexponentials, recent simulations have demonstrated that multiple-site hopping should result in a coverage-dependent surface diffusion coefficient.[53] In contrast, perfluoro-*n*-butane, *n*-butane and the other alkanes on Ru(001) display coverage-independent surface diffusion coefficients. Thus the multiple-site hopping mechanism is not entirely consistent with the larger surface diffusion preexponentials of alkanes and perfluoro-*n*-butane on Ru(001).

C. Coverage-independent diffusion

Measurements of surface diffusion and desorption provide direct information about the parallel and perpendicular surface potentials. At low adsorbate coverages, the activation energies are dominated by the adsorbate–surface interaction. As the adsorbate coverage is increased, adsorbate–adsorbate interactions may become important and can influence surface diffusion.[2,3,30,54] The surface diffusion of CO on Ru(001) was a clear example where repulsive nearest-neighbor interactions significantly influenced CO surface mobility.[10,11]

For perfluoro-*n*-butane on Ru(001), Fig. 4 reveals that the surface diffusion coefficient at 110 K was coverage-independent within the experimental error. The surface diffusion coefficient of *n*-butane on Ru(001) was also independent of coverage.[12] Similarly, recent measurements of *n*-propane, *n*-pentane and *n*-hexane on Ru(001) have revealed surface diffusion coefficients that were coverage-independent.[12] This behavior indicates that the parallel surface potential is dominated by adsorbate–surface interactions.

Recent simulations have been employed to evaluate the accuracy of the surface diffusion coefficients obtained by LITD measurements.[55-57] These studies have addressed the problems associated with fitting a constant diffusion coefficient to LITD refilling data derived from an adsorbate with a coverage-dependent surface diffusion coefficient. For perfluoro-*n*-butane and *n*-butane[12] on Ru(001), the surface diffusion coefficients are independent of coverage. Previous simulations have shown that fitting LITD refilling data with constant diffusion coefficients is accurate when the surface diffusion coefficient is independent of coverage.[30] Consequently, no difficulties are encountered in the analysis of the LITD diffusional refilling data for perfluoro-*n*-butane and *n*-butane on Ru(001).

V. CONCLUSIONS

This investigation explored the effects of fluorine substitution on the surface diffusion and desorption kinetics for a physisorbed molecule on a single-crystal metal surface. The surface diffusion and desorption kinetics for perfluoro-*n*-butane on Ru(001) were examined using laser-induced thermal desorption (LITD) and temperature programmed desorption (TPD) techniques. The surface diffusion displayed Arrhenius behavior and was coverage independent. The surface diffusion parameters for perfluoro-*n*-butane on Ru(001) were $E_{dif} = 2.9 \pm 0.3$ kcal/mol and $D_0 = 5.9 \times 10^{-2 \pm 0.2}$ cm^2/s. The desorption parameters were $E_{des} = 13.8 \pm 0.6$ kcal/mol and $\nu_{des} = 2.8 \times 10^{21 \pm 0.1}$ s^{-1}.

In comparison, the surface diffusion parameters for *n*-butane on Ru(001) were $E_{dif} = 3.5 \pm 0.2$ kcal/mol and $D_0 = 1.4 \times 10^{-1 \pm 0.2}$ cm^2/s. The desorption parameters for *n*-butane on Ru(001) were $E_{des} = 11.9 \pm 0.5$ kcal/mol and $\nu_{des} = 3.6 \times 10^{15 \pm 0.1}$ s^{-1}. The surface corrugation ratio was defined as $\Omega \equiv E_{dif}/E_{des}$. The corrugation ratio was determined to be $\Omega = 0.21$ for perfluoro-*n*-butane on Ru(001). In contrast, the corrugation ratio was $\Omega = 0.29$ for *n*-butane on Ru(001), and $\Omega \approx 0.30$ for other *n*-alkanes, cycloalkanes and branched alkanes on Ru(001).

The comparison between perfluoro-*n*-butane and *n*-butane indicates that fluorination lowers the surface corrugation ratio on Ru(001). Likewise, fluorination significantly increases the preexponential for desorption from Ru(001). This increase in the desorption preexponential was partially explained by the effect of fluorine substitution on the rotational and translational partition functions of perfluoro-*n*-butane. The lower surface corrugation ratio for perfluoro-*n*-butane was attributed to the larger van der Waals' radius of fluorine and the greater distance of the carbon backbone of perfluoro-*n*-butane from the Ru(001) surface.

ACKNOWLEDGMENTS

This work was supported by the National Science Foundation under Grant No. CHE-8908087 and by a Sponsored University Research Contract from the IBM Corporation. Some of the equipment used in this work was provided by the NSF-MRL program through the Center for Materials Research at Stanford University. M.V.A. thanks the Eastman Kodak Co. for a graduate fellowship. S.M.G. acknowledges the National Science Foundation for a Presidential Young Investigator Award and the A.P. Sloan Foundation for a Sloan Research Fellowship.

[1] G. Ehrlich and K. J. Stolt, Annu. Rev. Phys. Chem. **31**, 603 (1980).
[2] D. A. King, J. Vac. Sci. Technol. **17**, 241 (1980).
[3] D. A. King, in *Chemistry and Physics of Solid Surfaces, Vol. 2* (CRC, Boca Raton, FL, 1979).
[4] C. H. Mak, J. L. Brand, A. A. Deckert, and S. M. George, J. Chem. Phys. **85**, 1676 (1986).
[5] C. H. Mak, B. G. Koehler, J. L. Brand, and S. M. George, J. Chem. Phys. **87**, 2340 (1987).
[6] C. H. Mak, B. G. Koehler, J. L. Brand, and S. M. George, Surf. Sci. **191**, 108 (1987).
[7] C. H. Mak, J. L. Brand, B. G. Koehler, and S. M. George, Surf. Sci. **188**, 312 (1987).
[8] J. L. Brand, A. A. Deckert, and S. M. George, Surf. Sci. **194**, 457 (1988).
[9] C. H. Mak, A. A. Deckert, and S. M. George, J. Chem Phys. **89**, 5242 (1988).
[10] A. A. Deckert, J. L. Brand, M. V. Arena, and S. M. George, Surf. Sci. **208**, 441, (1989).
[11] A. A. Deckert, J. L. Brand, M. V. Arena, and S. M. George, J. Vac. Sci. Technol. A **6**, 794 (1988).
[12] J. L. Brand, M. V. Arena, A. A. Deckert, and S. M. George, J. Chem. Phys. **92**, 5136 (1990).
[13] M. V. Arena, A. A. Deckert, J. L. Brand, and S. M. George, J. Phys. Chem. **94**, 6792 (1990).
[14] C. H. Mak, B. G. Koehler, and S. M. George, J. Vac. Sci. Technol. A **6**, 856 (1988).
[15] E. D. Westre, M. V. Arena, A. A. Deckert, J. L. Brand, and S. M. George, Surf. Sci. **233**, 293 (1990).
[16] S. M. George, A. M. De Santolo, and R. B. Hall, Surf. Sci. **159**, L425 (1985).
[17] R. Viswanathan, D. R. Burgess, Jr., P. C. Stair, and E. Weitz, J. Vac. Sci. Technol. **20**, 605 (1982).
[18] B. Roop, S. A. Costello, D. R. Mullins, and J. M. White, J. Chem. Phys. **86**, 3003 (1987).
[19] D. R. Mullins, B. Roop, and J. M. White, Chem. Phys. Lett. **129**, 511 (1986).
[20] E. G. Seebauer, A. C. F. Kong, and L. D. Schmidt, J. Chem Phys. **88**, 6597 (1988).
[21] E. G. Seebauer, A. C. F. Kong, and L. D. Schmidt, J. Vac. Sci. Technol. A **5**, 464 (1987).
[22] M. M. Walczak, P. K. Leavitt, and P. A. Thiel, J. Am. Chem. Soc. **109**, 5621 (1987).
[23] M. M. Walczak, P. A. Thiel, Surf. Sci. **224**, 425 (1989).
[24] J. P. Cowin, D. J. Auerbach, C. Becker, and L. Warton, Surf. Sci. **78**, 545 (1978).
[25] G. Wedler and H. Ruhmann, Surf. Sci. **121**, 464 (1982).
[26] J. L. Brand and S. M. George, Surf. Sci. **167**, 341 (1986).
[27] L. E. Firment and G. A. Somorjai, J. Chem. Phys. **66**, 2901 (1977).
[28] P. A. Redhead, Vacuum **12**, 203 (1962).
[29] A. Gavezzotti, M. Simonetta, M. A. Van Hove, and G. A. Somorjai, Surf. Sci. **154**, 109 (1985).
[30] C. H. Mak and S. M. George, Surf. Sci. **172**, 509 (1986).
[31] T. E. Madey and J. T. Yates, Jr., Surf. Sci. **76**, 397 (1978).
[32] T. E. Felter, F. M. Hoffmann, P. A. Thiel, and W. H. Weinberg, Surf. Sci. **130**, 163 (1983).
[33] F. M. Hoffmann, T. E. Felter, P. A. Thiel, and W. H. Weinberg, Surf. Sci. **130**, 173 (1983).
[34] L. E. Firment and G. A. Somorjai, J. Chem. Phys. **69**, 3940 (1978).
[35] M. V. Arena and S. M. George (in preparation).
[36] T. M. Miller and B. Bederson, in *Advances in Atomic and Molecular Physics* **13**, 1 (1977).
[37] A. J. Hopfinger, *Conformational Properties of Macromolecules* (Academic, New York, 1973).
[38] F. O. Goodman, Phys. Rev. **164**, 1113 (1967).
[39] W. A. Steele, Surf. Sci. **36**, 317 (1973).
[40] K. J. Laidler, *Chemical Kinetics* (Harper & Row, New York, 1987).
[41] E. G. Seebauer, A. C. F. Kong, and L. D. Schmidt, Surf. Sci. **193**, 417 (1988).
[42] S. Nordholm, Chem. Phys. **98**, 367 (1985).
[43] L. Schmidt and R. Gomer, J. Chem. Phys. **42**, 3573 (1965).
[44] L. Holmlid and K. Möller, Surf. Sci. **149**, 609 (1985).
[45] M. J. Dresser, T. E. Madey, and J. T. Yates, Surf. Sci. **42**, 533 (1974).
[46] E. F. Green, J. T. Kelly, M. A. Pickering, and D. K. Stewart, Surf. Sci. **139**, 185 (1984),
[47] M. D. Scheer, R. Klein, and J. D. McKinley, J. Chem. Phys. **55**, 3577 (1971).
[48] C. G. Goymer and D. A. King, J. Chem. Soc. Faraday **68**, 280 (1972).
[49] H. Ibach, W. Erley, and H. Wagner, Surf. Sci. **92**, 29 (1980).
[50] J. C. Tracey, J. Chem. Phys. **56**, 2736 (1972).
[51] A. H. Smith, R. A. Barker, and P. J. Estrup, Surf. Sci. **136**, 327 (1984).
[52] D. Menzel, in *Interactions on Metal Surfaces*, edited by R. Gomer (Springer, New York, 1975), p. 101.
[53] M. V. Arena, A. A. Deckert, and S. M. George, Surf. Sci. (in press).
[54] M. Bowker and D. A. King, Surf. Sci. **71**, 583 (1978).
[55] M. C. Tringides, J. Chem. Phys. **92**, 2077 (1990).
[56] M. C. Tringides, Surf. Sci. **204**, 345 (1988).
[57] L. A. Ray, R. C. Baetzold, and J. Simon, Surf. Sci. **235**, 47 (1990).